

# Transient Stability Enhancement of Power System with Grid Connected DFIG Based Wind Turbine



D. Rakesh Chandra, Surender Reddy Salkuti,  
and Venkataramana Veeramsetty

**Abstract** Transient stability (TS) is one of the major issues of wind power grid integration. The reasons for transients are sudden severe disturbances such as faults. To save the grid from severe damage we must concentrate on transient stability management. A fixed-speed wind generator is easy to operate and reliable but it may not operate effectively under critical conditions such as transient stability. Coming to variable speed wind energy generators (WEGs) they can improve the TS of the system, and the Doubly Fed Induction Generator (DFIG) is one among the variable speed WEGs. In this work, the impact of DFIG on the TS of the power system connected to the grid has been investigated, and also rotor resistance control method is utilized to enhance the TS of the system. Here the proposed TS analysis has been implemented on a Reliability Test System (RTS)-24 bus system. All the simulation studies have been carried out in a MATLAB-compatible-based Power System Analysis Toolbox (PSAT) toolbox. From the obtained simulation studies it can be observed that in DFIG wind turbine addition of external resistance has improved system transient stability and the system could reach steady-state quickly as damping ratio is enhanced due to proportional relationship with the external resistance being added.

**Keywords** Renewable energy · Transient stability · Wind power · Induction generator · Power system

---

D. Rakesh Chandra  
Department of Electrical and Electronics Engineering, Kakatiya Institute of Technology and Science, Warangal, India  
e-mail: [drc.eee@kitsw.ac.in](mailto:drc.eee@kitsw.ac.in)

S. R. Salkuti (✉)  
Department of Railroad Electrical Systems, Woosong University, Daejeon 34606, Republic of Korea  
e-mail: [surender@wsu.ac.kr](mailto:surender@wsu.ac.kr)

V. Veeramsetty  
Center for Artificial Intelligence and Deep Learning, SR Engineering College, Warangal, India  
e-mail: [venkataramana\\_v@srecwarangal.ac.in](mailto:venkataramana_v@srecwarangal.ac.in)

## Nomenclature

TS	Transient stability
WEGs	Wind energy generators
DFIG	Doubly Fed Induction Generator
RTS	Reliability Test System
PSAT	Power System Analysis Toolbox
NN	Neural network
PLL	Phase-locked loop
MG	Microgrid
DDSG	Direct-drive synchronous generator
CSWT	Constant speed wind turbine
SCIGs	Squirrel Cage Induction Generators
GB	Gearbox
VSC	Voltage source converter

## 1 Introduction

Recently, power generation using renewable energy resources (RERs) is on an increase due to the considerations of green energy. At the beginning of 2020, the global installed RERs utility-scale capacity stood at 2537 GW with wind and solar PV combined contributing about 46% of the total global RERs share. In the modern world, energy has a strong relationship with the socio-economic development of a country. RERs are an adequate substitute for a conventional power system that can provide greener, consistent, quality power with low network congestion and losses. Wind energy availability is huge and it is eco-friendly. Nowadays, wind power generation has been increasing continuously throughout the world. Distributed generation in the form of RERs produces dependency on conventional energy generation and reduces the carbon footprint. Wind energy conversion system has several economic, technical, social, and environmental challenges. Economic challenges include high installation cost, technology challenges include power electronic converters (i.e., high power density converters and advanced cooling methods), controllers (pitch angle controllers, inverter-side, and grid-side converters). At present fixed and variable speeds, induction generators (IGs) are utilized for the generation of electrical power by using the wind source. Thus the integration of wind energy into the utility grid arise the issues such as rotor angle stability and transient stability (TS) problems.

In reference [1], a multilayered neural network (NN) is used to find the TS of the power system by using the PSAT software. A simple DFIG wind turbine along with its power converter model is simulated in [2] using DiGSILENT software to meet the power demand. Enhancement of both voltage stability and TS has been performed in reference [3] by using the wind energy converter with the help of P/Q control and modern voltage source converter (VSC). Comparisons among various

types of wind turbines according to their actual market share and cost-performance have been proposed in references [4, 5]. An approach to improve voltage stability by using a static compensator is proposed in references [6, 7]. The impacts of WEG on the voltage and TS of power grids are examined in reference [8] by determining the effect of variable and fixed speed grid-connected IGs on power systems voltage stability. The voltage stability of the system with grid-connected fixed and variable speed wind turbines has been investigated in reference [9]. The stability of grid-connected DFIG by taking into account the phase-locked loop (PLL) dynamics is proposed in reference [10].

The coordinated control of DFIG based WEG and the microturbine in a DC microgrid (MG) with the constant power load has been proposed in [11]. In reference [12], the performance of grid-connected DFIG based wind turbine system with gear-train backlash is analyzed. A nonlinear control method to coordinate DFIG based WEGs and static compensators in multi-machine power systems are proposed in [13]. Reference [14] presents various issues related to the stability of wind energy systems with variable speed in weak and strong grids. Reference [15] investigates the modeling and TS analysis of the integrated WEG system. Reference [16] presents a comprehensive review among three main types of wind turbines, i.e., direct-drive synchronous generator (DDSG), constant speed wind turbine (CSWT), and DFIG. The small-signal stability of a grid-connected power system with squirrel cage induction generator using a PSAT analysis with localization of Eigenvalues is proposed in reference [17]. The behavior of DFIG for grid disturbances has been simulated and validated in reference [18].

As wind energy exhibits both uncertainty and variability, wind generation cannot be dispatched on demand. It is also highly complex to forecast wind energy with precision. When it is used in combination with conventional sources, it poses a lot of challenges to grid operators in maintaining grid stability. Wind energy integration also poses challenges like power quality, effective load management in the power system. A few more issues such as power balance, wind power reserve management, and voltage control of the power system will also pose challenges to the system operator. Power quality is the deviation from original sinusoidal voltage and current waveforms such as flickers, harmonics, voltage sag, and swell. The objective of this work is to enhance transient stability (TS) of the DFIG connected system with the optimum rotor resistance control method. This work mainly concentrates on TS analysis and enhancement where it is a real challenging issue for grid-connected wind turbine systems. Time-domain simulation analysis will give the overall impact of transient stability on the system. The rotor resistance control method is used for the first time in this chapter to improve the TS of DFIG connected to the RTS-24 bus system. This chapter investigates the transient stability of the RTS 24 bus system when DFIG (at bus number 14) is connected to it. The detailed mathematical modeling of DFIG is also presented in this chapter. All these simulation studies are implemented in PSAT software of version 2.1.8.

The chapter is organized as follows: Sect. 2 describes detailed mathematical modeling of DFIG wind turbine and the implementation details of wind turbine

integrated models for TS analysis using PSAT software. The description of the Reliability Test System (RTS) 24 bus system is presented in Sect. 3. Section 4 presents the results and discussion. Lastly, the chapter is summarized in Sect. 5.

## 2 Modeling of Doubly Fed Induction Generator (DFIG)

Integration of wind power into utility grid via grid-connected wind turbines creates stability problems. These wind turbine generators are usually either Squirrel Cage Induction Generators (SCIGs) or Doubly Fed Induction Generators (DFIG) that use constant speed and variable speed wind turbines, respectively. The requirement of reactive power by the wind turbines causes voltage stability issues. This stability problem is also based on the amount of power integrated into the grid. The stability problem is mainly divided into small signal stability and TS. Small signal stability is due to the power system being subjected to a small disturbance that leads to small incremental change in system variables. TS is due to the power system being subjected to severe disturbances such as breaker and faults interruptions etc. In recent times the majority of wind energy generation is done by DFIG based wind turbines. The basic configuration and schematic view of DFIG are depicted in Fig. 1. The DFIG is mainly combined with a gearbox (GB), induction generator, and converter. In this work, a partial scale converter with the rating of 20% to 30% of DFIG is used so that the speed can be varied within  $\pm 30\%$  of the synchronous speed. A partial scale converter makes DFIG more attractive in terms of economical point of view [19]. Generally wound rotor (slip ring) induction generators are used as DFIG.

In Fig. 1, GB is the gearbox, GSC is the grid side converter and RSC is the rotor side converter. GB is having more turns to improve wind speed to connect DFIG [20]. RSC and GSC are used to regulate reactive power and slip power recovery.

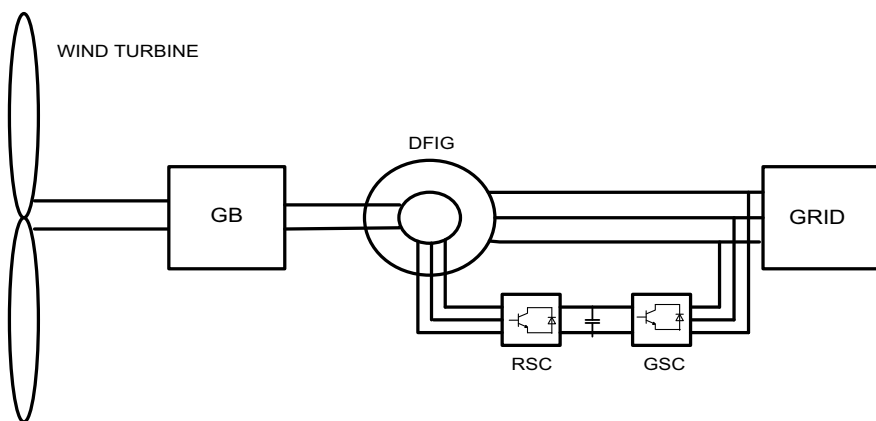


**Fig. 1** The basic configuration of DFIG

## 2.1 Mathematical Modeling of DFIG

Wind turbines with DFIG are used more often due to lower capital investment. DFIG is dominating the wind turbine market with a total share of 84.5% to 86%. Based on the operational characteristics, grid integration of wind turbines will lead to small signal or transient stability issues. For the same wind turbine rating, DFIG wind turbines have better reactive power regulation capability and transient voltage stability characteristics when compared to traditional induction generators. This section presents the mathematical modeling of DFIG. The steady-state expressions of DFIG are assumed and they are represented by,

$$v_{ds} = -r_s i_{ds} + [(x_s + x_m)i_{qs} + x_m i_{qr}] \quad (1)$$

$$v_{qs} = -r_s i_{qs} - [(x_s + x_m)i_{ds} + x_m i_{dr}] \quad (2)$$

$$v_{dr} = -r_R i_{dr} + (1 - \omega_m)[(x_R + x_m)i_{qr} + x_m i_{qs}] \quad (3)$$

$$v_{qr} = -r_R i_{qr} - (1 - \omega_m)[(x_R + x_m)i_{dr} + x_m i_{ds}] \quad (4)$$

In the above equations,  $x_m$  and  $x_s$  are magnetizing reactance and stator reactance respectively. Similarly  $x_R$  and  $r_R$  are rotor reactance and resistance respectively [21, 22].  $v_{ds}$ ,  $v_{qs}$  are the stator voltages of d and q axes. Similarly  $v_{dr}$ ,  $v_{qr}$  are the rotor voltages of d and q axes [23]. It may be noted that stator voltage mostly depends on the magnitude and phase angle, and they are expressed as,

$$v_{ds} = V \sin(-\theta) \quad (5)$$

$$v_{qs} = V \cos(\theta) \quad (6)$$

Here  $\theta$  is the angle between  $V$  and  $v_{qs}$ . The active power (P) and the reactive power (Q) that are injected into the utility grid depends on the stator and grid-side currents of the converter. These are expressed as [24],

$$P = v_{ds}i_{ds} + v_{qs}i_{qs} + v_{dc}i_{dc} + v_{qc}i_{qc} \quad (7)$$

$$Q = v_{qs}i_{ds} - v_{ds}i_{qs} + v_{qc}i_{qc} - v_{dc}i_{dc} \quad (8)$$

These can be rewritten by considering the grid-side converter and converter power equations and they are expressed as,

$$P_c = v_{dc}i_{dc} + v_{qc}i_{qc} \quad (9)$$

$$Q_c = v_{qc}i_{dc} - v_{dc}i_{qc} \quad (10)$$

Rotor side active power ( $P_r$ ) and reactive power ( $Q_r$ ) are

$$P_r = v_{dr}i_{dr} + v_{qr}i_{qr} \quad (11)$$

$$Q_r = v_{qr}i_{dr} - v_{dr}i_{qr} \quad (12)$$

Further, if the converter is assumed to be lossless then the active power ( $P_c$ ) and reactive power ( $Q_c$ ) on the converter side are  $P_c = P_r$  and  $Q_c = 0$ . Finally, the injected power into the grid is given by [25],

$$P = v_{ds}i_{ds} + v_{qs}i_{qs} + v_{dr}i_{dr} + v_{qr}i_{qr} \quad (13)$$

$$Q = v_{qs}i_{ds} - v_{ds}i_{qs} \quad (14)$$

where  $i_{ds}$ ,  $i_{qs}$  are the stator currents of the d and q axes, respectively.  $i_{dr}$  and  $i_{qr}$  are the rotor currents of the d and q axes, respectively. In the generator, the motion equation of a single shaft model is utilized. In this work, it can be considered that converter controls can filter the dynamics of the shaft. Therefore,

$$\dot{\omega}_m = (T_m - T_e)/2H_m \quad (15)$$

$$T_e = \psi_{ds}i_{qs} - \psi_{qs}i_{ds} \quad (16)$$

The stator flux and generator currents relationship can be expressed as,

$$\psi_{ds} = -[(x_s + x_m)i_{ds} + x_m i_{dr}] \quad (17)$$

$$\psi_{qs} = -[(x_s + x_m)i_{qs} + x_m i_{qr}] \quad (18)$$

$\psi_{ds}$  and  $\psi_{qs}$  are stator fluxes on the d-axis and q-axis respectively. Then, electrical torque ( $T_e$ ) is expressed as,

$$T_e = x_m(i_{qr}i_{ds} - i_{dr}i_{qs}) \quad (19)$$

The mechanical torque ( $T_m$ ) is given by [26],

$$T_m = \frac{P_w}{\omega_m} \quad (20)$$

## 2.2 *Implementation of Wind Turbine Integrated Models for TS Analysis Using PSAT Software*

Wind power grid integration creates stability problems. The world is facing a severe energy security problem with demand for energy going to be triple by 2050. Also, increasing restrictions on conventional energy sources to resist environmental change is giving rise to increased use of renewable resources for electricity production. Wind energy being uncertain and dynamically generates the issue of the storage facility when integrated into the grid. TS studies are addressed using PSAT which is MATLAB-compatible software. TS studies have been done by applying a 3 phase fault at time  $t = 3$  s and the duration of fault is 150 ms. The step-by-step procedure to implement the wind turbine integrated models for the TS analysis using PSAT [27, 28] is presented next:

- **Step 1:** Install PSAT software in MATLAB R2009a version.
- **Step 2:** Create the new data file (SIMULINK model) in PSAT (MATLAB compatible toolbox) by clicking File/Open/New data file.
- **Step 3:** Construct SCIG wind turbine integrated to IEEE 14 bus system model with 3 phase fault (at time  $t = 3$  s and fault clearing time is 50 ms) in MATLAB SIMULINK using PSAT library and save this file with a suitable name.
- **Step 4:** Give practical wind speed data as an input file to the wind turbine model by editing the PSAT data file (.m model).
- **Step 5:** Load the data file by clicking “File/Open/ datafile/select data file (from saved file)/load”.
- **Step 6:** After loading the data file, run power flow by clicking on the option “Power Flow” (for this select Newton–Raphson method which is available in settings).
- **Step 7:** After executing power flow, carry out time-domain simulation (for this select Trapezoidal method which is available in settings) by selecting the option as “Time Domain” and simulate for 20 s of time (for this keep ending time = 20 s). The system may reach a steady-state within 3–4 s. But to have further insight into system behavior the study period is extended to 20 s.
- **Step 8:** After time-domain simulation, plot the curves such as rotor angles, bus angles, and voltages, etc. for the time by clicking on the option “Plot” which is on the right side of the PSAT tool-bar.

## 3 Reliability Test System (RTS) 24 Bus Test System

In this chapter, an RTS-24 bus test system has been used for the TS analysis and the enhancement of grid-connected DFIG based wind turbine. This test system includes 10 generating units, one synchronous condenser, 4 transformers, and 38 transmission lines. These transmission lines have two different voltage levels, i.e., 230 and 138 kV. The 138 kV is in the lower portion whereas 230 kV is in the upper portion connected by 230/138 kV transformers at buses 11, 12, and 24. The wind turbine is connected

to RTS 24 bus system at bus number 14 as shown in Fig. 2. The total generation of all conventional generators is 2340 MW in the case of the RTS-24 bus system. As mentioned earlier, at bus number 14 wind turbine generator (i.e., DFIG) with the capacity of 240 MW (all wind turbines together) is integrated, which is more than 10% of total conventional generation. A three-phase fault was applied at the 11<sup>th</sup> bus at time  $t = 3$  s, and fault clearing time is set to 50 ms. In RTS 24 bus system, the wind turbines are connected at bus number 14 which has been chosen randomly. A 3-phase fault is applied at the 11th bus as shown in Fig. 2. The fault is applied at  $t = 3$  s and the fault clearing time is 50 ms.

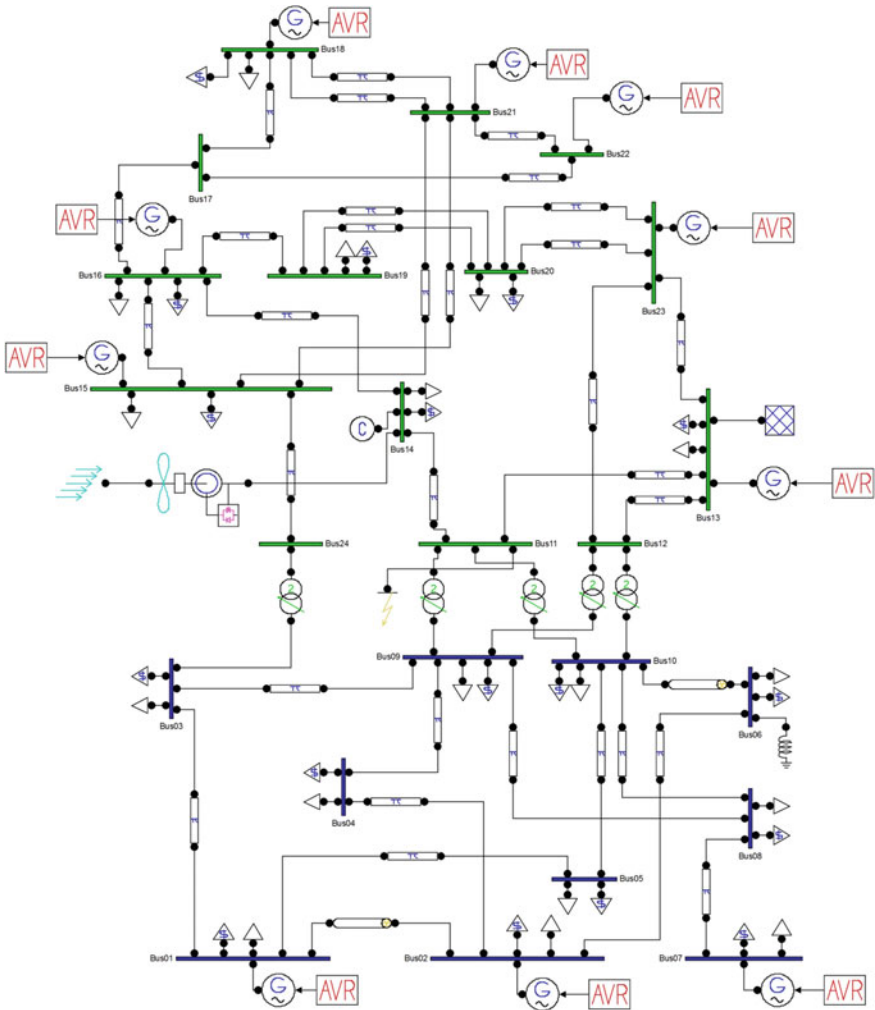


**Fig. 2** PSAT Simulated RTS 24 bus system with DFIG wind turbine at bus 14 and fault at bus number 11



### 4 Results and Discussion

The analysis of bus angles, rotational speeds of generators, generator rotor angles, and voltages at all buses have been discussed in this section. The test system used for the analysis is RTS 24 bus system with the integration DFIG wind turbine. Comparisons of all the results of transient stability study under severe fault conditions are also presented. DFIG wind turbines can supply the active power at constant frequency and voltage despite rotor speed variation.

After execution of power flow, time-domain simulation has been carried out for 20 s. The fault is applied at t equal to 3 s to evaluate system transient stability and fault is cleared at 50 ms. Figures 3, 4, 5 and 6 show the variation of rotor angles, angular speed, bus angles, and voltage magnitudes of DFIG wind turbine integrated RTS 24 bus system which is subjected to three-phase fault at bus number 11.

Figures 3, 4, 5 and 6 show that due to the application of the 3-phase fault at bus 11, the rotor angles have varied from 1 to 1.4 radians, and finally reached to steady-state as shown in Fig. 3. Figure 4 describes the variation of angular speeds in the range of 0.97–1.1 p.u and reached steady on the removal of a fault. Figures 5 and 6 indicate that bus angles reached 0.15 radians, the voltage dropped to 0.3 p.u during the fault and all these values have reached a steady-state after removing fault within simulated time. From the above analysis, it can be concluded that the system is stable.

In the DFIG wind generator, the maximum peak overshoot is less, and hence the steady-state is achieved in less time after clearing the fault. Further, with DFIG transient stability can be improved using the rotor resistance control method and is discussed in Sect. 4.1.

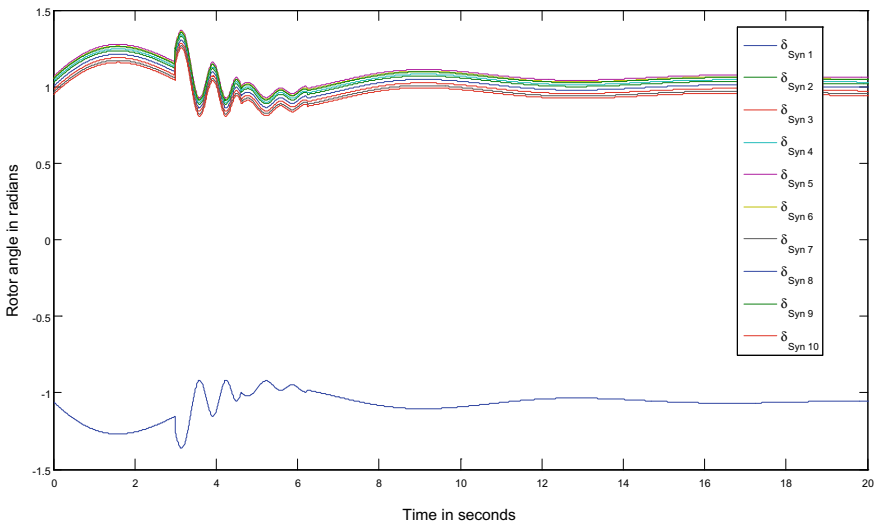


**Fig. 3** Rotor angles of different generators for 24 bus system with DFIG wind turbine, fault at bus 11

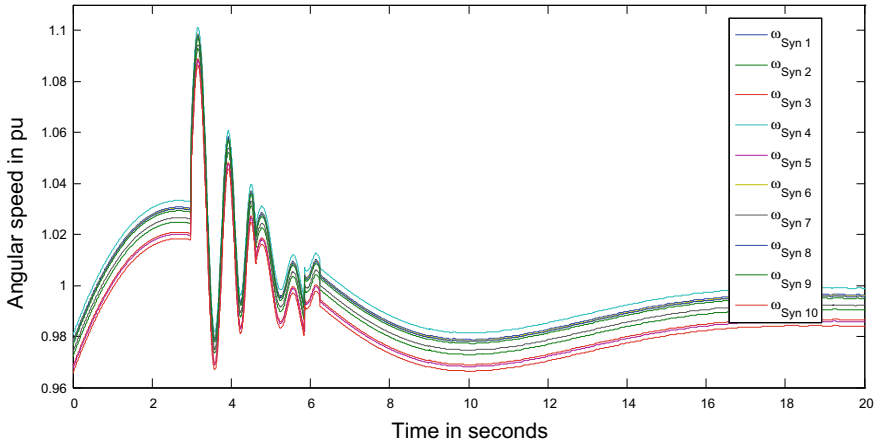


**Fig. 4** Angular speeds at different synchronous generators for 24 bus systems with DFIG wind turbine, fault at bus 11

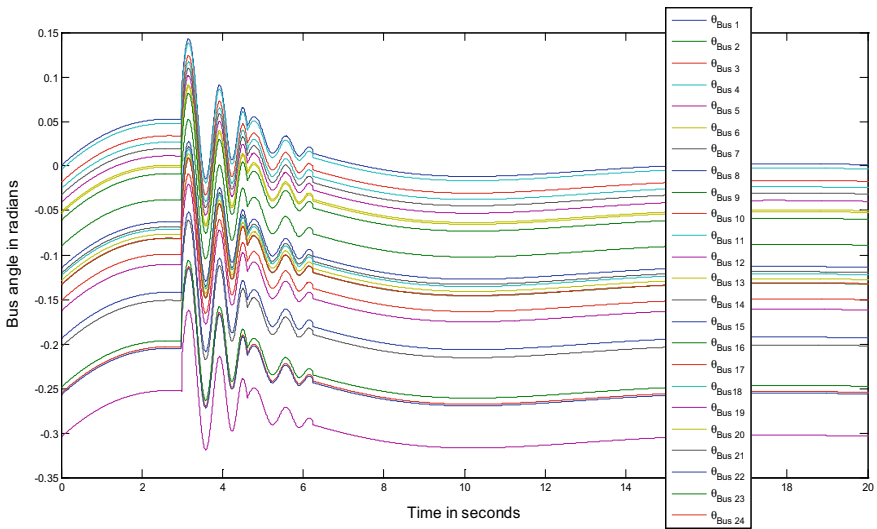


**Fig. 5** Bus angles at various busses for 24 bus system with DFIG, fault at bus 11

### 4.1 Transient Stability Enhancement of DFIG Integrated RTS 24 Bus System

TS enhancement is the process of improving the system damping and reducing the maximum peak overshoot and thereby helping the system to reach a steady-state quickly. For stability improvement, external rotor resistance (variable resistance) is

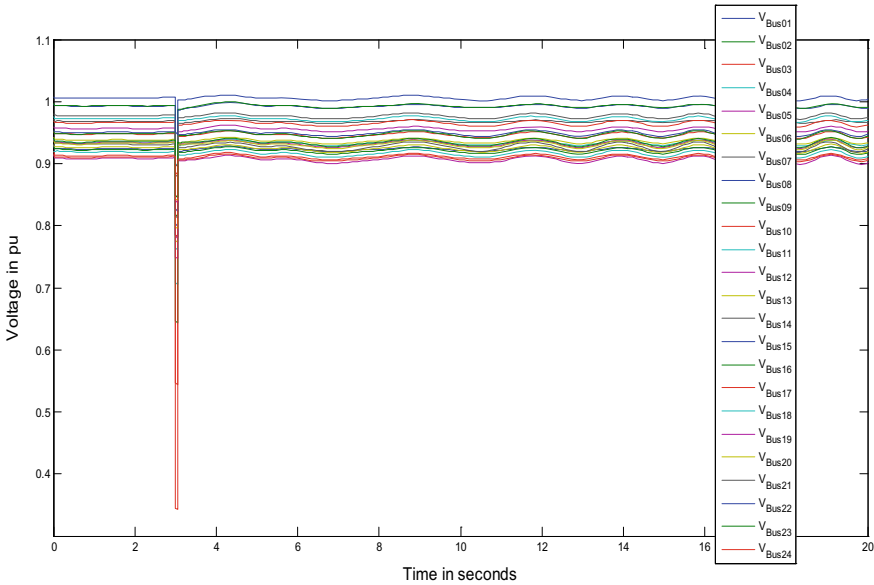
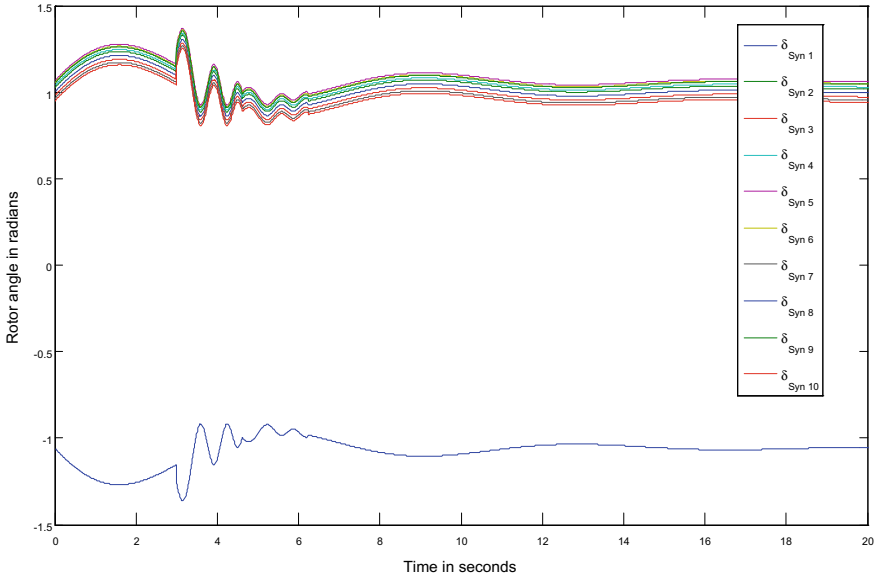


**Fig. 6** The voltage at various busses for 24 bus systems with DFIG, fault at bus 11

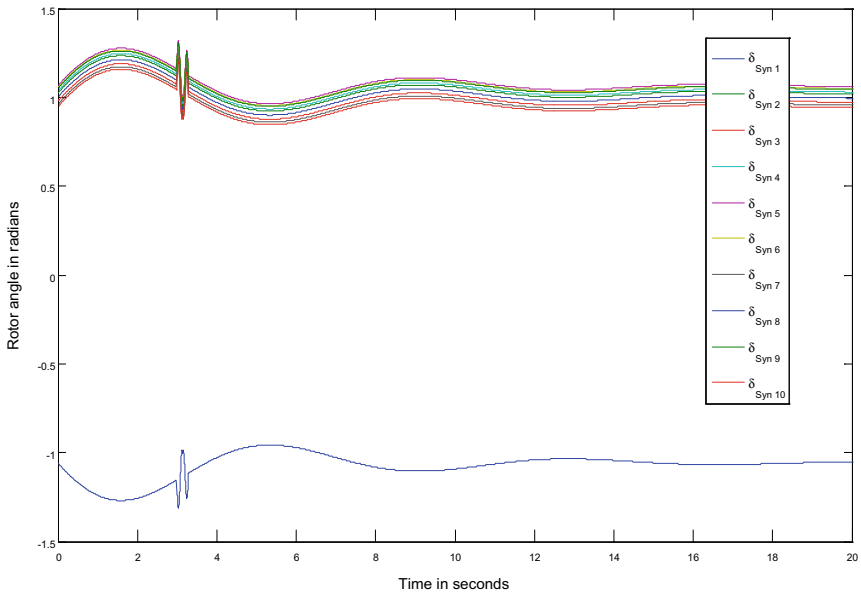
added on the rotor side which is possible in DFIG (slip ring) based wind turbines and this method is known as rotor resistance control. In this section rotor, the resistance control method is used to enhance the TS of the RTS 24 bus system. This is the usual practice in the case of a wound rotor (slip ring) induction generator to improve torque-slip controllability. In this method, an external resistor is added to the rotor windings through a power electronic converter. Adding external resistance on the rotor side causes more losses. So, resistance should be selected optimally to improve TS as well as considering losses. In the present work, external resistance is changed with different values and finally fixed at 50% of the original value. Studies are conducted on DFIG integrated RTS 24 bus system and results are discussed below. The rotor resistance has been modified from 0.01 to 0.015 p.u, and all other parameters remain unchanged in the waveforms shown below.

Figure 7 depicts the rotor angle enhancements with rotor resistance control of RTS 24 bus system, fault at bus 11. Figure 7a presents the rotor angle enhancements with  $R_s$  is 0.01 p.u,  $X_s$  is 0.10 p.u,  $R_r$  is 0.01 p.u and  $X_r$  is 0.08 p.u. Figure 7b presents the rotor angle enhancements with  $R_s$  is 0.01 p.u,  $X_s$  is 0.10 p.u,  $R_r$  is 0.015 p.u and  $X_r$  is 0.08 p.u. In Fig. 7, the maximum rotor angle is 1.4 radians (approximately) before adjustment of rotor resistance (from Fig. 7a) and after rotor resistance modification maximum rotor angle is limited to 1.3 radians (from Fig. 7b).

Figure 8 depicts the angular speed enhancements with rotor resistance control of RTS 24 bus system, fault at bus 11. Figure 8a presents the angular speed enhancements with  $R_s$  is 0.01 p.u,  $X_s$  is 0.10 p.u,  $R_r$  is 0.01 p.u and  $X_r$  is 0.08 p.u. Figure 8b presents the angular speed enhancements with  $R_s$  is 0.01 p.u,  $X_s$  is 0.10 p.u,  $R_r$  is

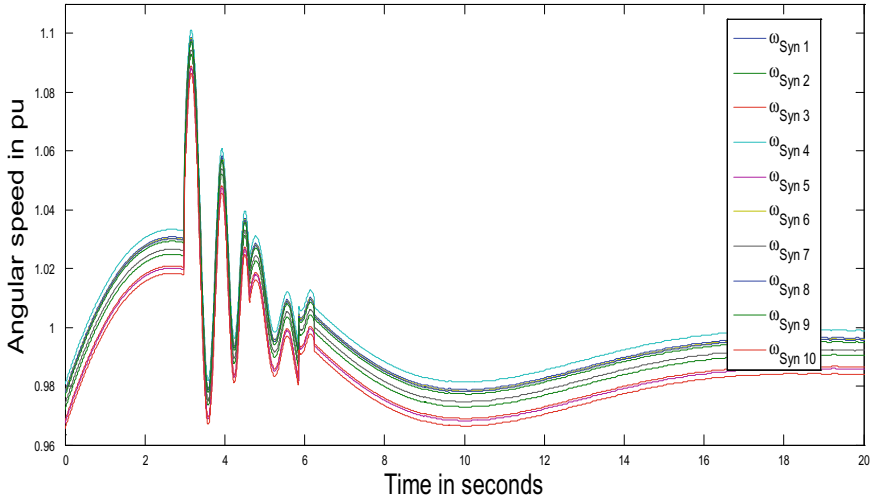


(a)

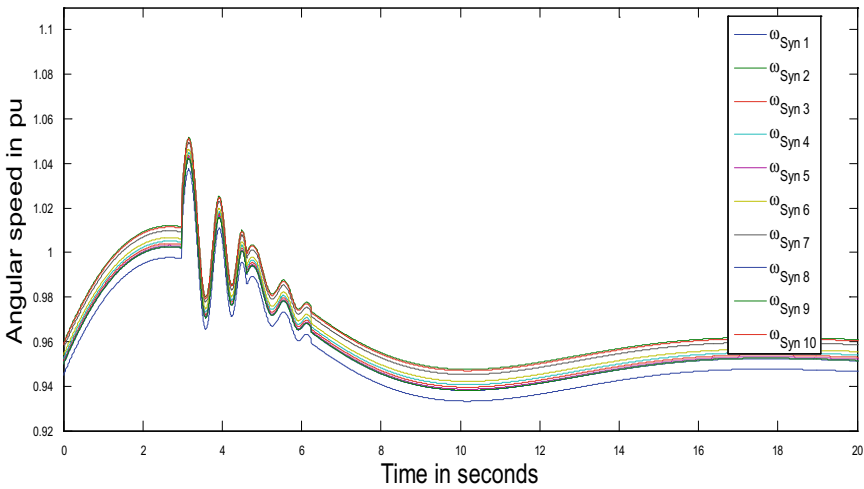


(b)

**Fig. 7** Rotor angle enhancements with rotor resistance control of RTS 24 bus system, fault at bus 11



(a)



(b)

**Fig. 8** Angular speed enhancements with rotor resistance control of RTS 24 bus system, fault at bus11

0.015 p.u and  $X_r$  is 0.08 p.u. In Fig. 8, the synchronous machine angular speed is 1.1 p.u before adjustment of rotor resistance (from Fig. 8a) and after modification of rotor resistance, it is less than 1.06 p.u (from Fig. 8b).

Figure 9 depicts the bus angle enhancements with rotor resistance control of RTS 24 bus system, fault at bus 11. Figure 9a presents the bus angle enhancements with  $R_s$  is 0.01 p.u,  $X_s$  is 0.10 p.u,  $R_r$  is 0.01 p.u and  $X_r$  is 0.08 p.u. Figure 9b presents the bus angle enhancements with  $R_s$  is 0.01 p.u,  $X_s$  is 0.10 p.u,  $R_r$  is 0.015 p.u and  $X_r$

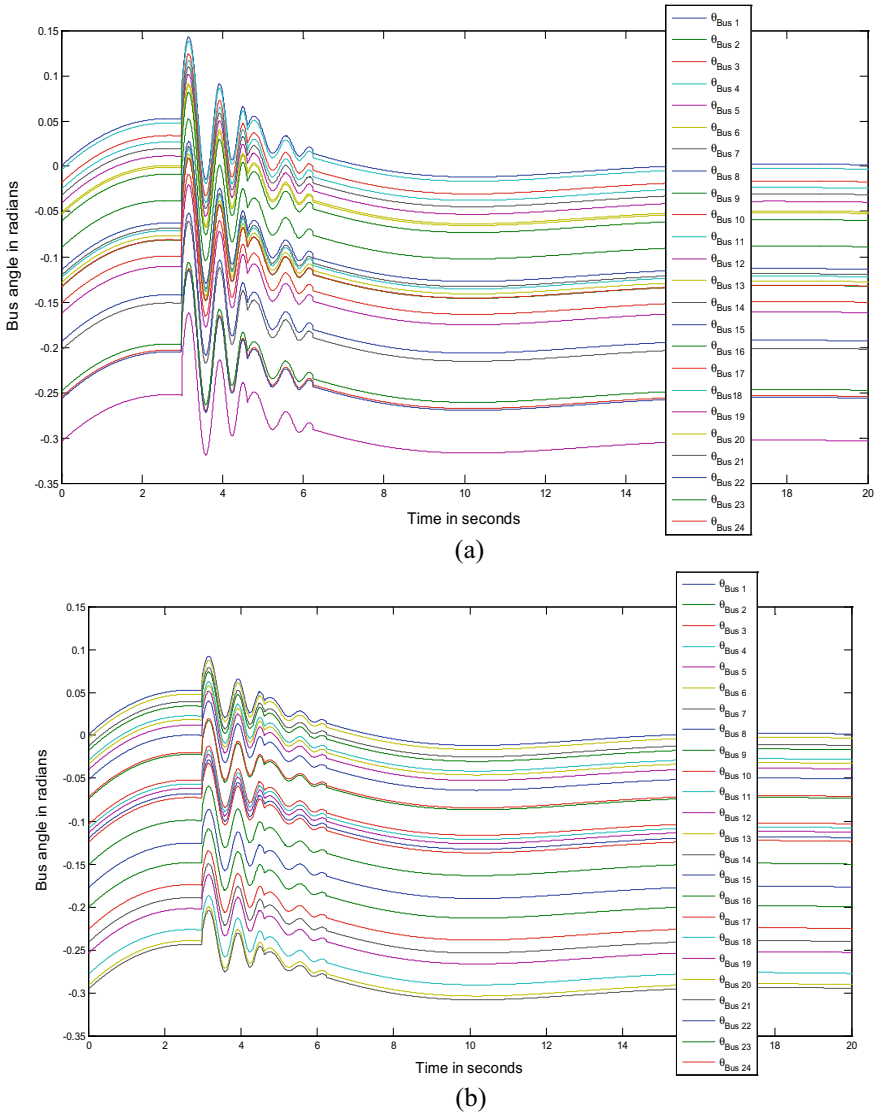


**Fig. 9** Bus angle enhancements with rotor resistance control of RTS 24 bus system, fault at bus 11

is 0.08 p.u. In Fig. 9, bus angles peak values are near to 0.15 radians with  $R_r$  is 0.01 p.u (from Fig. 9a) and 0.1 radians after adding external rotor resistance to 0.015 p.u (from Fig. 9b).

The above case studies on test systems conclude that an increase in rotor resistance improves the TS of the system. This is because of the proportionality of the damping ratio with the resistance. As the damping ratio of the system increases the maximum

peak overshoot and the oscillations of the system reduce thereby improving the TS of the system. After execution of power flow, time-domain simulation has been carried out for the 20 s. A fault is applied at  $t = 3$  s to evaluate system transient stability and fault is cleared at 50 ms. In DFIG wind turbine addition of external resistance has improved system transient stability and the system could reach steady-state quickly as damping ratio is enhanced due to proportional relationship with the external resistance being added.

## 5 Conclusions

This chapter presents the transient stability (TS) analysis of power systems by incorporating the wind energy generators by Power System Analysis Toolbox (PSAT) software. The detailed mathematical modeling of DFIG is also presented in this work. In DFIG, the control action is performed by using a power electronic-based converter that can be controlled by using rotor frequency, and hence the rotor speed. With the help of this converter, the DFIG can import or export the reactive power support from the main grid, and it has rotor-side control as well as power electronics-based control. These controlling methods make DFIG wind turbines efficient. Further, in DFIG wind turbine addition of external resistance has improved system transient stability and the system could reach steady-state quickly as damping ratio is enhanced due to proportional relationship with the external resistance being added. In the proposed TS analysis, rotor angle variation, rotational speeds of individual generators, bus voltages, and angles at all buses are analyzed. Simulation results are performed on the RTS-24 bus system. All the obtained results are visualized with graphical representation. It can be observed from the results that the deviations in the rotor angle are low in magnitude and can show better damping by using the DFIG. As time progresses, for the generator rotational speeds and voltage at individual busses, the oscillations, and maximum peak values have reduced in the case of DFIG. Wind power integration studies including the energy storage systems are the scope for future research work.

**Acknowledgements** This research work was funded by “Woosong University’s Academic Research Funding—2021”.

## References

1. Karami ESZ (2013) Transient stability assessment of power systems described with detailed models using neural networks. *Int J Electr Power Energy Syst* 45(1):279–292. <https://doi.org/10.1016/j.ijepes.2012.08.071>
2. Lei Y, Mullane A, Lightbody G, Yacamini R (2006) Modeling of the wind turbine with a doubly fed induction generator for grid integration studies. *IEEE Trans Energy Convers* 21(1):257–264. <https://doi.org/10.1109/TEC.2005.847958>

3. Ullah NR, Thiringer T (2007) Variable speed wind turbines for power system stability enhancement. *IEEE Trans Energy Convers* 22(1):52–60. <https://doi.org/10.1109/TEC.2006.889625>
4. Goudarzi N, Zhu WD (2013) A review on the development of wind turbine generators across the world. *Int J Dyn Control* 1:192–202. <https://doi.org/10.1007/s40435-013-0016-y>
5. Li H, Chen Z (2008) Overview of different wind generator systems and their comparisons. *IET Renew Power Gener* 2(2):123–138. <https://doi.org/10.1049/iet-rpg:20070044>
6. Thomas PC, Sreerenjini K, Pillai AG, Cherian VI, Joseph T, Sreedharan S (2013) Placement of STATCOM in a wind integrated power system for improving the load ability. In: *IEEE international conference on power, energy and control, Dindigul, India*, pp 110–114. <https://doi.org/10.1109/ICPEC.2013.6527633>
7. Buch H, Bhagiya RD, Shah BA, Suthar B (2011) Voltage profile management in restructured power system using STATCOM. In: *Nirma University international conference on engineering, Ahmedabad, India*, pp 1–7. <https://doi.org/10.1109/NUIConE.2011.6153279>
8. Muljadi E, Nguyen TB, Pai MA (2008) Impact of wind power plants on voltage and transient stability of power systems. In: *IEEE energy 2030 conference, Atlanta, GA, USA*, pp 1–7. <https://doi.org/10.1109/ENERGY.2008.4781039>
9. Devaraj D, Jeevajyothi R (2011) Impact of wind turbine systems on power system voltage stability. In: *IEEE international conference on computer, communication and electrical technology, Tirunelveli, India*, pp 411–416. <https://doi.org/10.1109/ICCET.2011.5762510>
10. Azizi AH, Rahimi M (2018) Dynamic performance analysis, stability margin improvement and transfer power capability enhancement in DFIG based wind turbines at weak ac grid conditions. *Int J Electr Power Energy Syst* 99:434–446. <https://doi.org/10.1016/j.ijepes.2018.01.040>
11. Akhbari A, Rahimi M (2020) Control and stability analysis of DFIG wind system at the load following mode in a DC microgrid comprising wind and microturbine sources and constant power loads. *Int J Electr Power Energy Syst* 117. <https://doi.org/10.1016/j.ijepes.2019.105622>
12. Prajapat GP, Senroy N, Kar IN (2018) Modeling and impact of gear train backlash on performance of DFIG wind turbine system. *Electr Power Syst Res* 163(A):356–364. <https://doi.org/10.1016/j.epsr.2018.07.006>
13. Morshed MJ, Sardoueinassab Z, Fekih A (2019) A coordinated control for voltage and transient stability of multi-machine power grids relying on wind energy. *Int J Electr Power Energy Syst* 109:95–109. <https://doi.org/10.1016/j.ijepes.2019.02.009>
14. Bhukya J, Mahajan V (2019) Optimization of damping controller for PSS and SSSC to improve stability of interconnected system with DFIG based wind farm. *Int J Electr Power Energy Syst* 108:314–335. <https://doi.org/10.1016/j.ijepes.2019.01.017>
15. Pillai AG, Thomas PC, Sreerenjini K, Baby S, Joseph T, Sreedharan S (2013) Transient stability analysis of wind integrated power systems with storage using central area controller. In: *IEEE international conference on microelectronics, communications and renewable energy*, pp 1–5. <https://doi.org/10.1109/AICERA-ICMiCR.2013.6575991>
16. Ouyang H, Li P, Zhu L, Hao Y, Xu C, He C (2012) Impact of large-scale wind power integration on power system transient stability. In: *IEEE international conference on innovative smart grid technologies*, pp 1–6. <https://doi.org/10.1109/ISGT-Asia.2012.6303130>
17. Lopez YU, Navarro JAD (2008) Small signal stability analysis of wind turbines with squirrel cage induction generators. In: *IEEE international conference on transmission and distribution conference and exposition, Bogota, Colombia*, pp 1–10. <https://doi.org/10.1109/TDC-LA.2008.4641779>
18. Petersson TT, Harnefors L, Petru T (2005) Modeling and experimental verification of grid interaction of a DFIG wind turbine. *IEEE Trans Energy Convers* 20(4):878–886. <https://doi.org/10.1109/TEC.2005.853750>
19. Kadri A, Marzougui H, Aouiti A, Bacha F (2020) Energy management and control strategy for a DFIG wind turbine/fuel cell hybrid system with super capacitor storage system. *Energy* 192. <https://doi.org/10.1016/j.energy.2019.116518>
20. Xiong L, Li P, Wu F, Ma M, Khan MW, Wang J (2019) A coordinated high-order sliding mode control of DFIG wind turbine for power optimization and grid synchronization. *Int J Electr Power Energy Syst* 105:679–689. <https://doi.org/10.1016/j.ijepes.2018.09.008>



21. Zhang T, Yao J, Pei J, Luo Y, Zhang H, Liu K, Wang J (2020) Coordinated control of HVDC sending system with large-scale DFIG-based wind farm under mono-polar blocking fault. *Int J Electr Power Energy Syst* 119. <https://doi.org/10.1016/j.ijepes.2020.105943>
22. Jerin ARA, Prabaharan N, Palanisamy K, Umashankar S (2017) FRT capability in DFIG based wind turbines using DVR with combined feed-forward and feed-back control. *Energy Proc* 138:1184–1189. <https://doi.org/10.1016/j.egypro.2017.10.233>
23. Gebru FM, Khan B, Alhelou HH (2020) Analyzing low voltage ride through capability of doubly fed induction generator based wind turbine. *Comput Electr Eng* 86. <https://doi.org/10.1016/j.compeleceng.2020.106727>
24. Yao J, Pei J, Xu D, Liu R, Wang X, Wang C, Li Y (2018) Coordinated control of a hybrid wind farm with DFIG-based and PMSG-based wind power generation systems under asymmetrical grid faults. *Renew Energy* 127:613–629. <https://doi.org/10.1016/j.renene.2018.04.080>
25. Adetokun BB, Muriithi CM, Ojo JO (2020) Voltage stability assessment and enhancement of power grid with increasing wind energy penetration. *Int J Electr Power Energy Syst* 120. <https://doi.org/10.1016/j.ijepes.2020.105988>
26. Hossain MdE (2017) Performance analysis of diode-bridge-type non-superconducting fault current limiter in improving transient stability of DFIG based variable speed wind generator. *Electr Power Syst Res* 143:782–793. <https://doi.org/10.1016/j.epsr.2016.09.020>
27. Okedu KE (2017) Augmenting DFIG wind turbine transient performance using alternative voltage source T-type grid side converter. *Renew Energy Focus* 18:1–10. <https://doi.org/10.1016/j.ref.2017.02.004>
28. Milano F (2005) Power system analysis toolbox. Version 1.3.4, software and documentation, July 14, 2005